International Journal of Disaster Risk Reduction 132 (2026) 105949

Contents lists available at ScienceDirect

International Journal of Disaster Risk Reduction

journal homepage: www.elsevier.com/locate/ijdrr

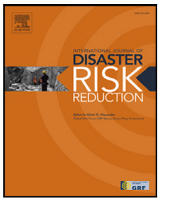

Prioritisation Recommendation Mapping (PrioReMap): A method for supporting relief coordination in flood disaster response

Moritz Schneider [a,*], Lukas Halekotte [a], Tina Comes [a,b], Frank Fiedrich [c]

[a] Institute for the Protection of Terrestrial Infrastructures, German Aerospace Center, Sankt Augustin, Germany
[b] Faculty of Technology, Policy and Management, TU Delft, Delft, The Netherlands
[c] Chair for Public Safety and Emergency Management, University of Wuppertal, Wuppertal, Germany

ARTICLE INFO

Keywords:
Spatial prioritisation
Flood management
Disaster risk reduction
Decision support
Bayesian network
GIS

ABSTRACT

To effectively coordinate the response to a flood disaster, decision-makers have to prioritise areas that are in most urgent need of assistance. This prioritisation often has to be carried out under time pressure and on the basis of incomplete information, creating a high cognitive load for decision-makers. Methods that integrate Bayesian networks into GIS to draw spatial inference can inform this prioritisation process. However, existing approaches are not equipped to address the time pressure and unclear information-scape that is typical for a flood disaster. In this work, we present a novel spatial inference method for area prioritisation that is designed to address these time and information constraints. The core of this method is a GIS-informed Bayesian network, integrated into an expected loss framework, that can be set up during the preparation phase. The method can then quickly provide area prioritisation recommendations for disaster relief, which has the potential to support decisions-makers during the response phase. In this way, our method provides a means of shifting some of the most time-consuming aspects of the decision-making process from the time-critical disaster response phase to the less critical preparation phase. To illustrate how our method can support rapid and transparent area prioritisation, we present a case study of an extreme flood scenario in Cologne, Germany.

1. Introduction

Flooding is among the most common and devastating natural hazards, posing severe threats to human life and critical infrastructures [1–3]. Due to climate change and urbanisation, the flood risk for urban areas has substantially grown in the recent past and is very likely to grow further in the future [4–7]. Therefore, cities around the globe need to develop appropriate strategies for dealing with an increasing flood disaster risk. One of the most demanding tasks in dealing with a disaster is the effective coordination of response efforts [8]. An effective response requires a rapid yet comprehensive assessment of the situation [9,10]. One crucial aspect of this assessment is the identification and prioritisation of the most impacted areas in the disaster zone, which helps to coordinate the rapid and efficient allocation of limited resources [11,12].

In the initial stages of a flood disaster, the actual impact of the event is often not exactly known or has not yet fully developed [9]. Effectively, this means that operational impact assessments need to be risk-based – they can only estimate where the impact is expected to be highest, based on available proxy data. Since disaster risk results from the intersection of hazard, exposure, and vulnerability [13–15], all three dimensions need to be considered when identifying and prioritising at-risk areas. This includes, for instance, the spatial distribution of the hazard intensity [16], the density of residential buildings [17], the accessibility of

* Corresponding author.
E-mail address: moritz.schneider@dlr.de (M. Schneider).

https://doi.org/10.1016/j.ijdrr.2025.105949
Received 6 June 2025; Received in revised form 24 November 2025; Accepted 2 December 2025
Available online 3 December 2025
2212-4209/© 2025 The Authors. Published by Elsevier Ltd. This is an open access article under the CC BY license (http://creativecommons.org/licenses/by/4.0/).

critical infrastructures (CI) [18,19], and the location of vulnerable people [20]. Accordingly, decision-makers have to handle a large amount of different and potentially volatile pieces of information [21,22]. On top of this, there is the issue that, especially at the onset of a flood, the available information tends to be uncertain [23], particularly in terms of human adaptive behaviour [24]. This combination of versatile and numerous but also volatile and fragmentary information has been shown to result in cognitive overload on decision-makers that can hamper their capacity to manage disaster response efforts efficiently [25,26].

A suitable tool for reducing the cognitive load on decision-makers are decision support systems that consider the available information, process it, and present it in a concise manner. In the context of flood disaster risk reduction, a combination of geo-information systems (GIS) and Bayesian networks (BNs) has been proven to provide valuable support for *long-term* decision making, e.g. for informing flood mitigation by identifying flood prone areas [27,28], or flood protection by assessing potential CI failures [29,30]. By combining a GIS with a BN, area-specific assessments that include a variety of spatially distributed variables can be conducted (e.g. see [14] or [27]). In this context, the popularity of BNs stems from three aspects that are particularly critical in disaster-related contexts: (i) BNs can be constructed based on diverse compositions of available data, e.g. a combination of historical data and expert knowledge [31], (ii) BNs are explainable and easy to interpret as they are based on a (logical) graphical structure [32], and (iii) BNs enable the consideration of uncertainties in input data and relations between variables [33] – which is crucial to avoid overconfidence when making high-stake decisions in uncertain situations [23].

Existing GIS-informed BN models are designed to inform strategic decisions in disaster risk reduction. As a result, they are not equipped to support the decision-making process in flood disaster response, which is characterised by the tension between temporal urgency and the complexity of the situation. However, BN-based approaches are generally well suited to address the particularities of disaster situations. A BN-based approach, designed to reflect the cognitive process that leads to disaster response decisions, can be utilised to draw some of the more time-consuming aspects of the decision-making process out of the time-critical disaster response phase and treat them during model development, which can be carried out in the preparation phase. This involves addressing questions regarding (i) the variables that are critical for disaster risk, (ii) the dependencies between these variables, (iii) the level of risk that justifies area prioritisation, and (iv) the treatment of uncertainties in the available information. Properly treating these questions is a non-trivial and time-consuming task that must take into account different needs and thus may require consultation with multiple experts [34]. Accordingly, holding appropriate discussions when time permits and moulding the results into a comprehensible model (that is the BN) can help decision-makers to make faster, better justified, and thus more confident decisions when time is short.

In this work, we present a novel method called *PrioReMap* (Prioritisation Recommendation Mapping) that supports decision-maker in coordinating relief measures in the event of flood disasters. The method includes two layers that together constitute the contribution of our work: (i) a novel area prioritisation method that is informed by (ii) a novel GIS-informed BN model that is tailored to the information-scape in an ongoing flood disaster. The resulting recommendations can help decision-makers allocate scarce resources to priority areas or to select appropriate locations for temporary storage, shelters, field hospitals, or command centres.

In the remainder of this paper, we first provide the background on GIS-informed BN models, especially in the context of flood disasters (see Section 2). Based on the literature, we derive design properties of such models. We demonstrate the need for a new approach based on these design properties via a stylised case (see Section 3). Subsequently, we present our method for area prioritisation (see Section 4). We illustrate the effectiveness of our *PrioReMap* method in a case study of a flood scenario in Cologne, Germany (see Section 5). Finally, the proposed method is discussed and future work is outlined (see Section 6).

2. Background: GIS-informed Bayesian networks

The combination of GIS and Bayesian networks has become increasingly popular for spatial inference. For instance, GIS-informed BN have been applied to optimise the placement of charging stations for electric vehicles [35], to find the most suitable sites for pumped hydro energy storage [36], to evaluate the suitability of underground space as a resource for urban development [37], or to identify suitable areas for timber production under conservation constraints [38]. In disaster risk reduction, this approach has frequently been applied for creating risk maps, e.g. for fire [39], avalanches [40], or ecological risk [41]. GIS-informed BN models are particularly well established in the context of flood disaster risk reduction (see Table 1 for an overview).

Although the objective of GIS-informed BN can differ, their construction tends to follow three general design properties (DP1-DP3):

DP1 – Discrete target node represents the analysis objective. The first step in constructing a GIS-informed BN is the specification of a target node that reflects the objective of the analysis (see Table 1). For example, [14] present a BN-based approach to identify areas of high flood disaster risk, which is reflected in the target node *Flood Disaster Risk*. The possible outcomes of the analysis are then set by the states that this target node can adopt. In all applications of GIS-informed BN for flood risk, the target nodes show discrete states, which can be (i) binary states, such as *Yes* and *No* or *True* and *False*, or (ii) higher granularity state descriptions, such as *High*, *Medium*, and *Low* (see Table 1). The motivation for using discrete instead of continuous states is that models in this context are often primarily built from expert knowledge, and discrete states are often easier to elicit from experts.

DP2 – Study area is divided into sub-areas. To develop the GIS models, the study area must be divided into smaller subset areas that are individually assessed. To achieve this, the area can be divided by using regular tiles, such as squares (e.g. see [14]) or spatially distributed components, such as buildings (e.g. see [23]). These subset areas determine the resolution of the subsequent analysis.

Table 1
GIS-informed BN models for flood disaster preparedness in the literature.

References	Analysis objective	Target node	Target node states	BN leaf nodes
[29]	Analysis of hospital service disruptions	Emergency Care	True, False	Flood Depth at Hospital, Accessibility, Power Supply Grid
[14]	Flood disaster risk assessment	Flood Disaster Risk	Extreme High, High, Moderate, Low, Very Low	Inundation Extent, River Network Density, River Buffering, Population Vulnerability, Economic Vulnerability, Building Vulnerability
[27]	Integrated flood risk assessment in data-scarce mega-cities	Flood Hazard Probability	Yes, No	Remote Sensed Urban Structure Types, Proximity to Large Scale Green Infrastructure, Topography, Proximity to River, Proximity to Coast
[42]	Flood risk assessment for road infrastructures	Flood Risk Factor	Low, Medium, High	Extreme Precipitation Susceptibility Index, Historical Records, Repair Cost, Light Traffic, Population Density, Soil, River Density
[43]	Disaster-causing factor chains on urban flood risk	Inundation	Yes, No	Elevation, Population Density, Annual Rainfall
[30]	Quantify resilience of roadways network infrastructure	Resilience	Low, Medium, High	Reliability, Recovery (of road network components)
[28]	Assessing urban flood disaster risk	Flood Disaster	Yes, No	River Density, Proximity, Elevation, Impervious Area, Per Unit GDP, Road Density, Population Density, Rainfall Duration
[44]	Assessing benefits of early warning systems	Vulnerability	Low, Medium, High	Emergency Personnel, People Risk Awareness, Reliability

DP3 – Leaf nodes are informed by GIS models. The target node, which is decomposed through one or more layers of parent nodes, leads to independent leaf nodes that are ultimately informed by the area-specific GIS models. For example, the target node *Flood Disaster Risk* in [14] has three parent nodes called *Hazard*, *Exposure*, and *Vulnerability*, which, in total, depend on six parent (leaf) nodes. Using the example of node *Exposure*, which has two parent (leaf) nodes called *River Network Density* and *River Buffering* that are ultimately informed by two individual GIS models. For each individually assessed area, spatially explicit information on all BN leaf nodes must be provided. When informing the area-specific BN leaf nodes with geospatial data, two cases of evidence must be distinguished: hard evidence and soft evidence. Hard (or regular) evidence describes a deterministic value that gives the exact state of a leaf node. Soft evidence, on the other hand, describes a probability ratio of a leaf node.

3. Motivation and main requirements - from layers to decision support

Based on the aforementioned basic design properties (**DP1-DP3**) of GIS-informed BN models in the literature (see Section 2), we construct a simple (low-dimensional) example model to illustrate how even a basic example yields results that can become difficult to comprehend – a critical issue especially under time pressure.

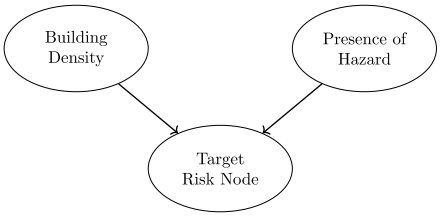

Building Density	Presence of Hazard	Target Risk Node		
		High	Medium	Low
High	True	1.00	0.00	0.00
High	False	0.00	0.00	1.00
Medium	True	0.75	0.25	0.00
Medium	False	0.00	0.00	1.00
Low	True	0.25	0.50	0.25
Low	False	0.00	0.00	1.00

Fig. 1. Low-dimensional BN model composed of the directed acyclic graph (left side) and CPT (right side).

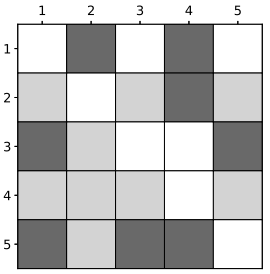

(a) Homogeneous spatial data.

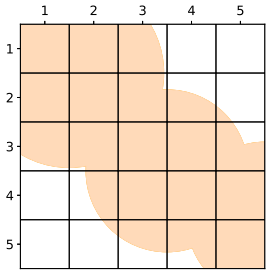

(b) Heterogeneous spatial data.

Fig. 2. Example GIS-data on a 5*x*5 matrix. Fig. 2(a) shows (homogeneous) building density geo-data in each cells with three configurations (high density in dark-grey, medium density in light-grey, and low density in white) processed as hard evidence. Fig. 2(b) shows geo-data that is not too tightly bound to the boundary of the cell processed as soft evidence.

The BN of this example features a *Target Risk Node* with three states (*High, Medium*, and *Low*) (following **DP1**) and two parent nodes (see left side of Fig. 1): (i) a node *Building Density* with three states (*High*, *Medium*, and *Low*); and (ii) a node *Presence of Hazard* with two states (*True* and *False*). The corresponding conditional probability table (CPT) attached to the *Target Risk Node* follows a simple structure: Given the presence of the hazard, cells with a high building density are most likely to obtain a high risk, followed by those with a medium building density, and those with a low building density (see right side of Fig. 1). As a geographical setup, we introduce a 5 × 5 matrix (see Fig. 2) with 25 cells (following **DP2**). Each cell of the matrix represents one subset area, i.e. the BN is duplicated and assigned to each cell. The two leaf nodes of each BN are informed by individual GIS layers (following **DP3**). The node *Building Density* is informed by a layer containing geo-data of the density of residential buildings that is assumed to be homogeneous in each cell (see Fig. 2(a)) and processed as hard evidence in the BN. The node *Presence of Hazard* is informed by a layer containing geo-data of the hazard distribution that is not tight to the boundaries of the cells (not homogeneous in every cell, see Fig. 2(b)) and processed as soft evidence in the BN.

The GIS-informed BN model provides probabilities for each cell to be in a state of *High*, *Medium*, or *Low* risk. Based on the corresponding heatmaps (Fig. 3), tendencies of high risk areas can easily be identified, especially in comparison to having only the two layers of geo-data (see Fig. 2). Accordingly, the model is already capable of reducing the cognitive load on potential decision-makers.

Looking more closely at the results, they reveal one cell that stands out with a 100% probability of high risk (see cell in row one, column two, i.e. cell (1,2), in Fig. 3). While this cell should clearly be prioritised when considering only the high risk matrix, cells (3,5) and (4,5) also show similarly high probabilities of high risk (~80%). However, the two cells differ in their remaining probability distribution: in cell (3,5), the remaining ~20% is assigned to low risk, whereas in cell (4,5), it is assigned to medium risk. As a result, the probability distribution of cell (4,5) can be considered more critical, despite having the same probability for the most severe (*High*) state (*Issue I*) – this example underscores the importance of taking the entire probability distribution into account when prioritising cells. A different prioritisation issue becomes apparent when comparing cells (2,1) and (3,1). While cell (3,1) exhibits a slightly higher probability of high risk (~84% vs. 75%), cell (2,1) shows a higher probability of medium risk (25% vs. 0%). As a result, the prioritisation depends on whether emphasis is placed solely on high risk or on a combination of high and medium risk levels, i.e. the prioritisation depends on the decision-maker's preferences (*Issue II*).

To conclude, while the presented low-dimensional example demonstrates the general suitability of a GIS-informed BN model for area prioritisation, it also highlights issues associated with applying this method in time-critical response efforts. Even though the entire setup is very simple, quickly comprehending the results (*Issue I*) and choosing a set of cells to prioritise (*Issue II*) is still not straightforward and can lead to a high cognitive load (especially under time pressure) as well as discrepancies in prioritisation among different responders — this is where our proposed method aims to enhance the literature by offering precise recommendations for area prioritisation. We argue that these recommendations should be based on the entire probability distribution of the target node (rather than solely on the most severe state), in order to further reduce cognitive load (thus avoiding *Issue I*) and to promote consistency in recommendation outcomes across responders by introducing a transparent expected loss framework (thus avoiding *Issue II*).

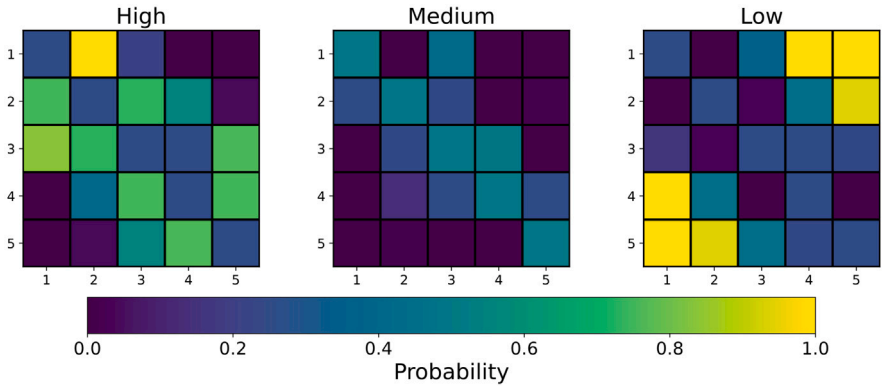

Fig. 3. Heatmaps presenting the state probabilities of the *Target Risk Node* (see Fig. 1) calculated using the cell-specific geo-data (see Fig. 2) to inform the cell-specific BN leaf nodes.

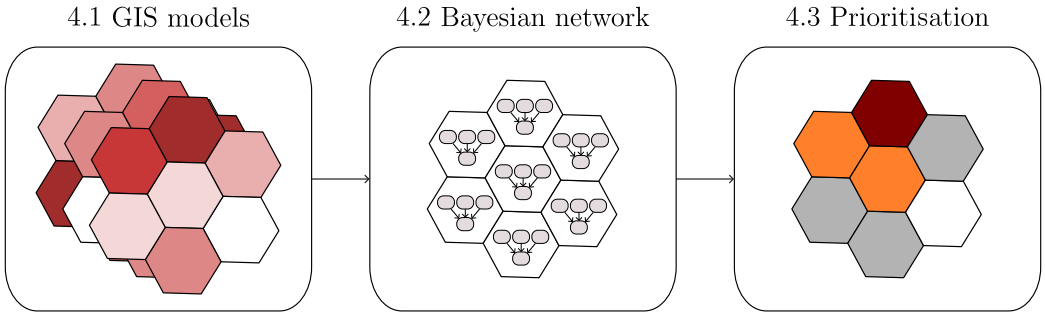

Fig. 4. Summary of the *PrioReMap* method. The method is structured in three stages: the development of tile-specific spatial models that represent the variables used for prioritisation, the construction of a BN that formalises the cognitive process of assessing risk based on these variables, and the prioritisation procedure that generates the final prioritisation recommendations.

4. Method: Prioritisation Recommendation Mapping (PrioReMap)

The method presented here is designed to support responders in prioritising areas in an ongoing flood disaster where the risk to people is high. It is composed of three main components (see Fig. 4): (i) the GIS models to provide spatially explicit observations of the critical variables characterising the *Hazard*, *Exposure*, and *Vulnerability* in a flood disaster risk scenario (see Section 4.1); (ii) the Bayesian network used to infer the probability of the target node called *Risk of People in Need of Assistance* based on the critical variables (see Section 4.2); and (iii) the prioritisation method that translates the probability distribution of the target node into prioritisation recommendations (see Section 4.3). When applying the method in disaster response, information about the current flood is fed into the corresponding GIS and then processed by the BN and the expected loss-based prioritisation method to compute the area prioritisation recommendations.

4.1. GIS models

The GIS models capture the spatial variables most relevant for assessing flood disaster risk and ultimately for prioritisation. The development of these models follows two consecutive steps: first, the tiling of the case study area, a procedure essential for operationalising the spatial resolution at which prioritisation is carried out. Second, the individual GIS models, each providing a tile-specific assessment of the critical variables used for prioritisation.

4.1.1. Hexagonal tiling

To enable the prioritisation of individual subset areas, i.e., specific zones within the broader disaster area, the study area is divided into a grid composed of uniform hexagon tiles (see Fig. 5). Hexagonal tiling is a well-established practice in geospatial applications, as it ensures uniform neighbour distances, reduces edge effects, and provides a consistent spatial representation [45]. For this purpose, the H3 system is utilised, a geospatial indexing system that partitions the Earth's surface into hexagonal tiles at multiple resolutions [46]. Each hexagon at every resolution is assigned a unique index key, allowing every tile to be readily identified. Since H3 is widely adopted across domains, including disaster response (e.g. see [12]), it further facilitates applicability of the method. The suggested resolution applied in the method presented is resolution 9, where each cell covers approximately $0.1\,\mathrm{km}^2$, which captures neighbourhood-level detail.

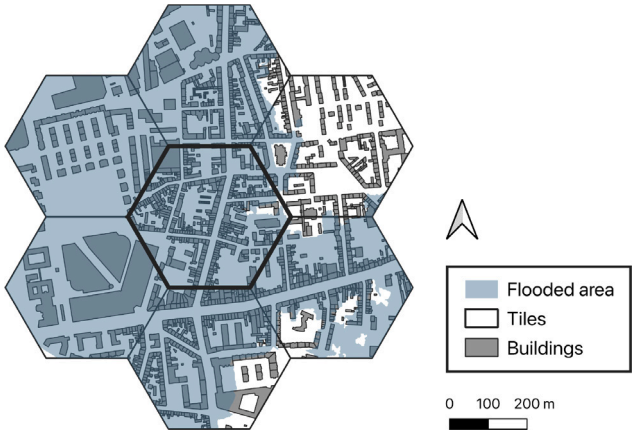

Fig. 5. Example hexagon including neighbouring hexagons.

4.1.2. Individual models

In the following, the GIS-based models representing the variables characterising the *Hazard*, *Exposure*, and *Vulnerability*, which together constitute the key contributors to *Risk of People in Need of Assistance* during a flood, are presented, along with typical thresholds describing their severity (these thresholds are later used for variable discretisation). Each assessment or analysis outlined corresponds to an individual tile.

The following variables characterise the (flood) *Hazard*. A first key variable is the *Flood Depth*. This variable is critical to assessing flood risk because water depth directly determines both potential damage and life-threatening conditions. It is represented by the maximum flood depth within a tile, which serves as a practical summary measure of severity (particularly in combination with the following variable). Two critical thresholds are applied: a depth of 30 cm, cited as the point at which the ground surface is no longer visible [47] and streets no longer passable [48,49], and a depth of 150 cm, at which damage to, e.g., buildings can become severe [47].

A second important variable is the *Flood Coverage* [14], defined as the proportion of the tile surface that is inundated. This variable is critical to assessing flood risk because the extent of inundation determines how much of the built and natural environment is exposed. It complements flood depth in characterising overall flood hazard severity.

The following variables characterise the *Exposure*. One central variable is the *Population*, i.e., the number of people living within a tile [28,42]. This variable is critical to assessing flood risk because it indicates how many people may be directly affected in a flood event. The information is derived from census data, which provides an approximated population count on a $100\,\mathrm{m} \times 100\,\mathrm{m}$ grid. To obtain tile-level values, the centroids of the census grid cells are assigned to the hexagonal tiles in which they fall, and the respective counts are aggregated per tile. Although the census and hexagonal grids do not align perfectly, the higher granularity of the census grid ($0.01\,\mathrm{km}^2$ compared to $0.1\,\mathrm{km}^2$ for the hexagonal grid) ensures sufficient precision for this aggregation. Because absolute population numbers can differ considerably between study areas (e.g., a maximum of 100 people per tile in a small town versus more than 1000 in a large city), relative measures are required. For this purpose, the 70th and 95th percentiles are used to identify tiles with comparatively high population concentrations within each study area.

A further relevant variable is the presence of *Points of Interest (PoI)*, which capture locations where large numbers of people may be present during daytime. This variable is critical to assessing flood risk because such facilities can greatly increase potential exposure during specific times of day. These include schools, care facilities, and tourist attractions, as well as critical infrastructures such as train stations. Here, only the presence or absence of one or more PoI are determined per tile. The location of these PoI can, for example, be obtained from OpenStreetMap (OSM).

The following variables characterise the *Vulnerability*. An essential variable is the *Access Road*, which describes the accessibility of a tile via the road network. This variable is critical to assessing flood risk because evacuation options strongly influence the vulnerability of affected populations. The accessibility is modelled using an adapted version of the accessibility model presented in [29]. To this end, the road network of the study area is reconstructed using OSM data [50], resulting in a network topology that features nodes representing road crossings and edges representing road segments [48]. Road segments that show a flood depth of more than 30 cm [48,49] are assumed to be impassible and are thus excluded from the topology. We assume that each remaining road segment can be used for evacuation purposes regardless of any traffic regulations such as one-way streets. For the routing algorithm, we defined multiple destination locations (places to escape to) that are sufficiently distant from flooded areas and which are very well connected to the road network to assess whether one can, in general, escape from a tile to a distant, unexposed area via the road network. To minimise potential biases introduced by the destination location, multiple locations are necessary.

A second variable of importance is the *Access Local*, i.e., the proportion of unexposed area in the immediate surroundings of a tile. This variable is critical to assessing flood risk because nearby safe areas directly determine short-term evacuation opportunities. It is estimated by calculating the percentage of the flooded area of all neighbouring tiles (see Fig. 5).

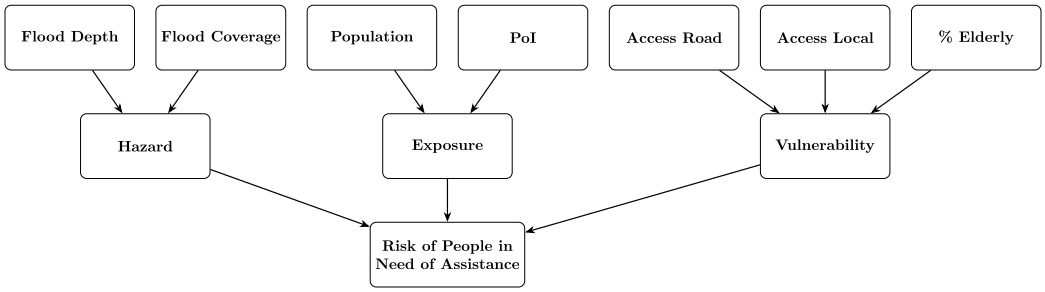

Fig. 6. Bayesian network to infer the *Risk of People in Need of Assistance*. The BN is composed of eleven variables (four conditional nodes and seven marginal nodes).

Finally, the percentage of elderly (*% Elderly*) is another decisive variable, as elderly citizens tend to require more assistance during evacuation in flood disasters [51,52]. This variable is critical to assessing flood risk because elderly populations often face greater difficulties in evacuation. It is determined by calculating the proportion of residents aged 67 years and older (obtained from the census data) relative to the total population within a tile.

4.2. Bayesian network

The BN represents the spatial inference model that integrates all tile-specific information into the posterior probability distribution of the target node *People in Need of Assistance*, which is essential for allocating relief resources. The BN reflects the cognitive process [53] of deriving this inference from all available information and enables its application to all tiles in a timely manner. In the following, we first outline the graphical structure of the BN, i.e., its nodes and edges, then describe the method used to populate the CPTs. Finally, we introduce the approach for handling observations provided by the spatial models, i.e., how they are considered as evidence for the leaf nodes of the BN.

4.2.1. Directed acyclic graph

The graphical structure of the BN follows a hierarchical organisation, where the leaf nodes correspond to the spatial models, i.e., each leaf node is informed by a single spatial model. In line with the structure proposed by [14], the BN specifies three child nodes – *Hazard*, *Exposure*, and *Vulnerability* – which represent the contributors to disaster risk [15]. The leaf nodes are grouped under these child nodes, with each leaf node serving as a parent of the factor it informs. Together, these three child nodes determine the single target child node, the *Risk of People in Need of Assistance* (see Fig. 6).

4.2.2. Conditional probability tables

Setting up the CPTs of a BN is widely recognised as one of the main challenges in their application, as this process can require a large number of probability values [31]. Since our aim is to reflect the cognitive process of an emergency responder, it is essential that expert knowledge can be easily incorporated and that the procedure for defining the CPTs remains transparent. To meet this requirement, all variables in the BN are discretised, meaning they are represented by discrete states even when the underlying variable is continuous in nature (e.g., flood depth). Threshold-based discretisation substantially reduces the number of probability values required, as each CPT must specify one value for every combination of parent-node states and child-node states. This approach is well established in domains where expert knowledge plays a central role and/or data availability is limited (see the references in Table 1).

In order to further facilitate the elicitation and provide a transparent support method, an adapted approach of the ordered logistic regression (ordered-logit) model proposed by [54] is used. This approach provides a structured way to translate qualitative parent states into quantitative probabilities for an ordered categorical child node C (i.e. nodes *Hazard*, *Exposure*, *Vulnerability*, and *Risk*). The process unfolds in three steps. First, each variable V has a finite set of ordered states $S_V = \{s_1, \dots, s_{K_V}\}$, which are mapped to a severity score between 0 (least severe) and 1 (most severe) using a severity mapping function

$$x_V : S_V \to [0, 1]. \tag{1}$$

This allows categorical states to be represented numerically in a consistent and interpretable manner – e.g., the parent *Flood Depth* might assign scores of 0.00 to *none*, 0.33 to *shallow*, 0.67 to *moderate*, and 1.00 to *deep*, so that being in the state *moderate* corresponds to a severity of 0.67. Second, when a child node C depends on multiple parents $\mathcal{P}(C) = \{P_1, \dots, P_m\}$, the individual severity scores of their current states $\mathbf{s} = (s_1, \dots, s_m)$ are combined into a single aggregated severity measure

$$\eta_C(\mathbf{s}) = \sum_{j=1}^{m} w_{C,P_j}\, x_{P_j}(s_j), \qquad \sum_j w_{C,P_j} = 1, \tag{2}$$

where the weights w_{C,P_j} represent the relative importance of each parent and are normalised to sum to one. Finally, this aggregated severity is linked to the probability distribution over the child's ordered states via the ordered-logit model. With slope parameter β_C and a sequence of thresholds $\tau_{C,1} < \cdots < \tau_{C,K_C-1}$, the cumulative probability of the child being in state k or below is

$$\Pr(Y_C \le k \mid \eta_C) = \sigma\big(\beta_C(\tau_{C,k} - \eta_C)\big), \qquad \sigma(z) = \frac{1}{1+e^{-z}}. \tag{3}$$

Subtracting consecutive cumulative values gives the probability of each specific category, thereby completing the corresponding CPT of the child node. All model parameters used to apply the order-logic method for the presented BN can be found in Appendix A.

4.2.3. Observation handling

While discretising a continuous variable into states is required to facility expert knowledge elicitation for CPT construction, it introduces sharp threshold effects, where a minimal change in a value provided by a spatial model could shift the evidence from 100% *moderate* to 100% *deep*. To enhance the robustness of the BN model against such threshold effects, soft evidence is applied by distributing probability mass smoothly across the discrete bins (which correspond to the variable states). Given an observation d^*, the weight for each bin i with edges $[b_i, b_{i+1})$ is computed as

$$w_i = \int_{b_i}^{b_{i+1}} \mathcal{N}(x; d^*, \sigma^2)\, dx, \tag{4}$$

where

$$\mathcal{N}(x; d^*, \sigma^2) = \frac{1}{\sqrt{2\pi\sigma^2}} \exp\!\left(-\frac{(x-d^*)^2}{2\sigma^2}\right) \tag{5}$$

is the normal density, and σ controls how gradual the transition is between bins. These weights, which sum to one, are entered as soft evidence in the BN rather than hard evidence. For example, for the node *Flood Depth* with states {none, shallow, moderate, deep} defined by cut points $\{0.0, 0.1, 0.5, 1.5\}$ m, an observed value $d^* = 0.49$ m with $\sigma = 0.1$ m yields approximate weights [0.01, 0.65, 0.34, 0.00], indicating that shallow flooding is most plausible but moderate flooding remains possible, with no abrupt jumps at the bin boundaries.

4.3. Prioritisation

The BN provides a probability distribution p_r over the risk states $R = \{\text{None}, \text{Low}, \text{Med}, \text{High}\}$ of the target node *Risk of People in Need of Assistance* for each tile. To translate the probabilistic output of the BN into concrete prioritisation recommendations, we apply an expected loss framework. This approach has been used in the literature to derive action recommendations from probability distributions (e.g., [55,56]). In this way, the decision process combines probabilistic reasoning with a cost-based criterion to balance probability and consequence.

The idea of the expected loss framework is to compare different candidate actions $a \in A$ in terms of the loss that will be incurred if they are chosen. In the context of disaster response, this loss can be quantified using *allocation-equivalent hours*, defined as the delay in hours by which relief resources arrive after the critical time threshold. To this end, risk states R of the BN target node are associated with deadlines T_r that specify the maximum acceptable delay for allocating relief resources. In the context of flood response, [57] provides an overview of the timeframes of decisions and needs assessments after floods. In addition, we draw on the *Report on Field-Based Decision-Makers Information Needs from the Digital Humanitarian Network* to derive and calibrate the thresholds [58]. On the basis of these references, indicative thresholds are assumed: about 24 h for urgent first aid (high risk areas), around 72 h for rapid needs assessment (medium risk areas), and up to one week for less urgent cases (low risk areas). The action set $A = \{\text{Immediate}, \text{Deferred}, \text{Extended}\}$ corresponds to three urgency levels aligned with the risk states: an *Immediate* action recommends mobilisation within $t_{\text{Immediate}} = 24$ h, a *Deferred* action within $t_{\text{Deferred}} = 72$ h, and an *Extended* action within $t_{\text{Extended}} = 168$ h. Thus, for an action $a \in A$ with response time t_a and a state $r \in R$ with maximum acceptable delay T_r,

$$\text{over-allocation}(a, r) = \max\big(t_a - T_r,\, 0\big), \tag{6}$$

and

$$\text{under-allocation}(a, r) = \max\big(T_r - t_a,\, 0\big) \tag{7}$$

is defined. Under-allocation captures the penalty of exceeding the required response time (too late), while over-allocation captures the cost of committing resources earlier than strictly necessary, which may reduce efficiency by preventing their use in more time-critical locations. The overall loss is

$$L(a, r) = \rho \cdot \text{under-allocation}(a, r) + (1-\rho) \cdot \text{over-allocation}(a, r), \tag{8}$$

where ρ is the tuning parameter that balances the penalty between under-allocation and over-allocation, with $\rho = 0.5$ describing equal penalties, $\rho = 1$ meaning only under-allocation is penalised, and $\rho = 0$ meaning only over-allocation is penalised. We introduced this parameter to reflect the fact that under-allocation (i.e., responding too late) is typically more critical in disaster response and should

therefore be penalised more severely. Although values smaller than 0.5 are technically feasible, they imply penalising over-allocation more heavily than under-allocation, which might not be meaningful in practical applications. The expected loss is then

$$EL(a) = \sum_{r \in R} p_r \, L(a, r). \tag{9}$$

In this formulation, rather than committing to a single most likely state, each possible action $a \in A$ is evaluated over the entire probability distribution by computing its expected loss. This ensures that uncertainty is explicitly incorporated: states with higher probability contribute more strongly, while even low-probability states influence the outcome if their associated costs are severe. For each tile the *critical delta*

$$\delta_i = EL(\text{Extended})_i + EL(\text{Deferred})_i - EL(\text{Immediate})_i \tag{10}$$

is computed, which quantifies the relative advantage of assigning tile i to the *Immediate* action. Sorting all tiles by δ_i in descending order yields a stable, deterministic queue. Selecting the top K tiles minimises the total expected loss under the constraint that K tiles are prioritised as *Immediate*. The parameter K – the *target count* – can be specified in multiple ways depending on planning needs: as an absolute number of tiles (e.g. $K = 200$), as the number of square kilometres covered (e.g. $4\,\text{km}^2$ resulting in a tile resolution dependent K), or as a percentage of the exposed disaster area (e.g. 20% resulting in a study area dependent K). The top K tiles are recommended for *Immediate* action, while the remainder are recommended for *Deferred* action. Subsequent waves are defined by consecutive blocks of size K in this global ranking, providing a transparent and interpretable prioritisation sequence for phased response under limited resources.

The set of tiles classified as *Immediate* can also be updated dynamically at run-time. There are two potential causes for an update: (i) new observations may become available that change the underlying risk probability distribution p_r, which in turn modifies the expected losses and queue ordering; or (ii) once a certain number of *Immediate* tiles have been inspected, the same number of tiles from the head of the remaining queue can be promoted to *Immediate*, thereby maintaining the target count K while ensuring continuous allocation of resources.

5. Application of PrioReMap: A case study of a flood disaster in Cologne, Germany

We illustrate the *PrioReMap* method in a flood scenario in Cologne, a German city with more than one million inhabitants [29]. In the past, the city of Cologne has proven to be vulnerable to river floods. For instance, in 1993 and 1995, the city experienced floods with severe consequences for its inhabitants and the local economy [59,60]. The city's vulnerability stems from its immediate proximity to the Rhine river which runs right through the densely populated city centre. Recently, the importance of an effective flood risk management in this region has been demonstrated by the flood disaster in the Ahr Valley in 2021 [61,62].

The case study is intended to showcase how the *PrioReMap* can be applied during a flood response. We choose data that resembles the information that is typically available during an ongoing flood. For the flood hazard layer (that includes the flood extent and depth), we use data from a hydrological simulation of an extreme flood scenario (also called 500-year flood or HQ500 [63]), which is typically used to create flood risk maps and inform flood protection planning (e.g. see [64]). As this dataset has the same structure as flood hazard layers generated by rapid mapping technologies, it could easily be replaced with the most recent snapshot of the flood to capture its temporal evolution during an actual event. For the assessment of the population density, we use census data at a $100\ \text{m} \times 100\ \text{m}$ resolution, which provides both the total number of people in each cell and demographic details, such as the number of individuals older than 67 years. Furthermore, we use OSM data that comprises building locations, PoI locations, and the road network. As it is reasonable to assume that this information does not change over the course of a flood event, there is no need to replace it with real-time data. However, the data should be checked for accuracy and completeness before being transferred to a real-world application.

5.1. Model results

5.1.1. GIS models

The first spatial model, which provides observations on the flood hazard, reveals that 2044 tiles are flooded, ranging from 0.01 to 100 percent coverage (Fig. 7(a)). The second model, analysing the maximum flood depth per tile, shows values ranging from 4 cm to 12.75 m (Fig. 7(b)). The model analysing the presence of people (contributing to the assessment of exposure) indicates that 2283 tiles are populated, with up to 2933 individuals per tile (Fig. 8a()). In 790 tiles, at least one PoI is present (Fig. 8(b)). The spatial models assessing vulnerability show that 666 tiles are rendered inaccessible due to flooded road segments (Fig. 9(a)), while 2574 tiles have at least one neighbouring tile flooded, up to cases where all neighbours are fully flooded (Fig. 9(b)). Finally, in 1917 tiles, people aged 67 and older are present (Fig. 9(c)).

5.1.2. GIS-informed BN models

Using the results of the GIS models (see Section 5.1.1) as inputs for the tile-specific BNs (see Section 4.2), the probability distribution for the states of the target node *Risk of People in Need of Assistance* is calculated for each flooded tile in the study area (see Fig. 10).

The results reveal several spatial clusters of tiles with high probability of the *High* state: 80 tiles have probabilities exceeding 75%. Two large clusters occur on both sides of the Rhine in the city centre (coinciding with the centre of Fig. 10(a)), along with a

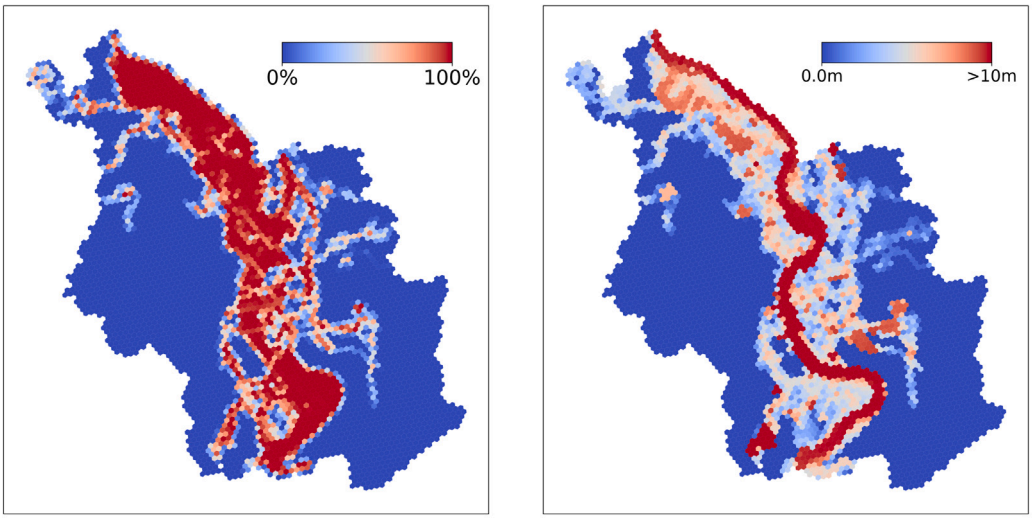

(a) Flood Coverage. (b) Flood Depth.

Fig. 7. Spatial models hazard.

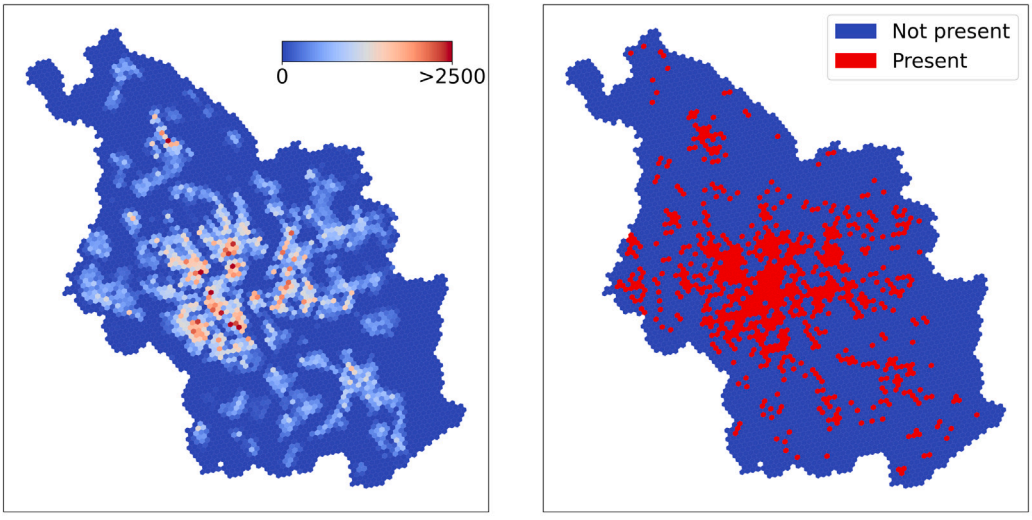

(a) Population. (b) PoI.

Fig. 8. Spatial models exposure.

small cluster in the north and another in the south. Probabilities for the *High* and *None* states range from 0 to about 80%, whereas those for *Medium* and *Low* range from 0 to about 50%. This pattern reflects the ordered-logit model, which tends to accentuate the extreme categories (*High* and *None*). A probability of 100% for the *High* state is not reached because no tile simultaneously exhibits the maximum flood depth and the maximum population density in the case study. Likewise, a probability of 100% for the *None* state is not observed because only tiles with some flood coverage are analysed.

5.2. Prioritisation recommendations

As a potential configuration for the final *PrioReMap*, the wave size is set to $K = 200$, which given 1096 exposed tiles, yields five full prioritisation waves plus a final partial wave. The penalty parameter ρ is set to 0.75, making under-allocation penalised three times more strongly than over-allocation. The resulting *PrioReMap* (Fig. 11) explicitly depicts the first and second prioritisation waves; for simplicity and accessibility, the remaining waves are summarised — it should be noted that this constitutes an example

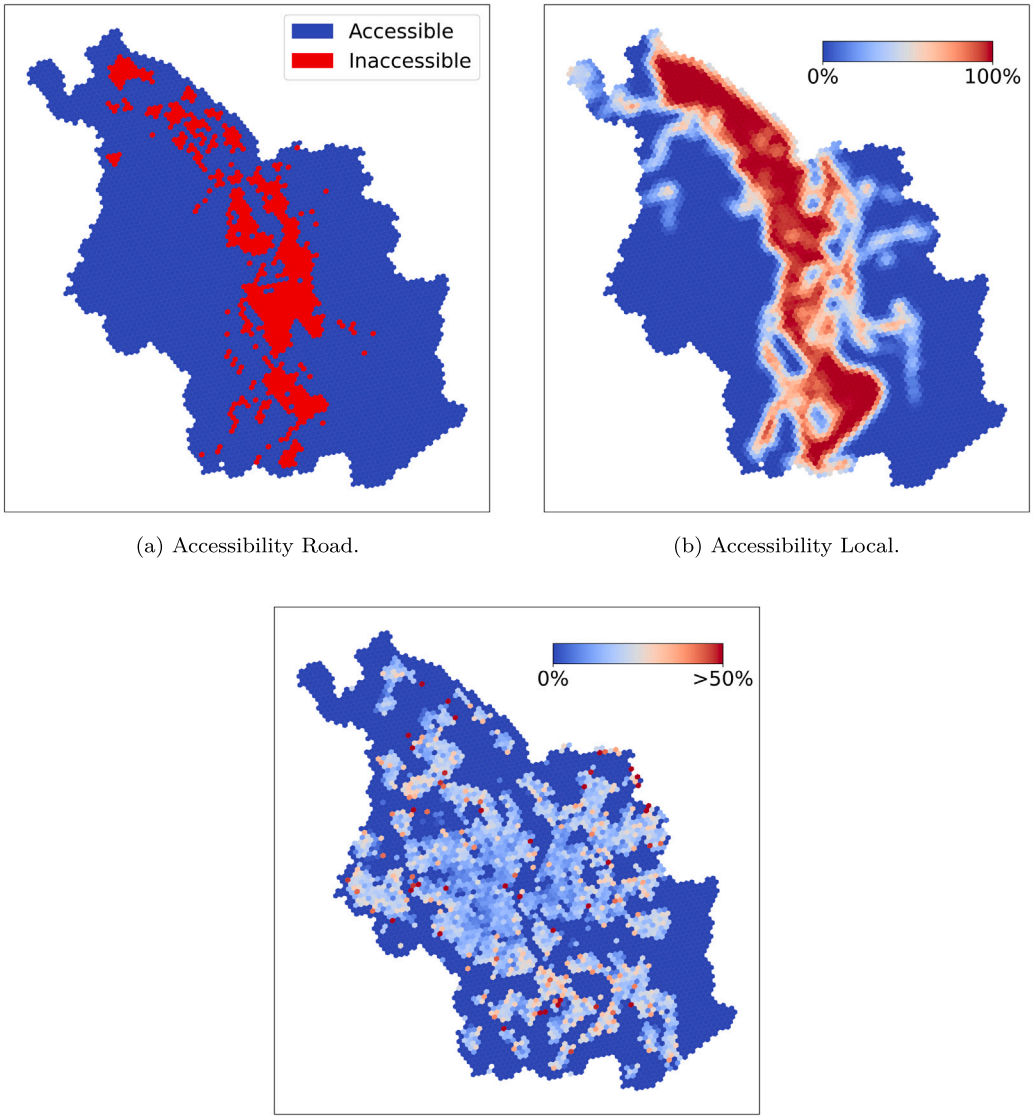

(a) Accessibility Road.

(b) Accessibility Local.

(c) % Elderly.

Fig. 9. Spatial models vulnerability.

visualisation, which can be adapted to user preferences. The first prioritisation wave exhibits several dense clusters, alongside a small number of isolated tiles. Tiles in the second prioritisation wave frequently surround those in the first, while also forming a few smaller stand-alone clusters as well as some isolated tiles.

A sensitivity analysis on variations of the penalty parameter ρ, together with an additional corresponding illustration of the *PrioReMap* of the case study, is provided in Appendix A.

6. Discussion

In this paper, we introduce *PrioReMap*, a novel method that provides area prioritisation recommendations in flood disaster response. The method consists of three core elements. First, a grid of BNs used to infer the spatially distributed *Risk of People in Need of Assistance* based on spatial variables, such as the population density and the accessibility of unexposed areas. Second, GIS models that inform the leaf nodes of the tile-specific BNs in the grid using a flood hazard layer. Third, a prioritisation method that translates the tile-specific probability distributions of the *Risk of People in Need of Assistance* into distinct prioritisation recommendations.

A central motivation for developing our *PrioReMap* method was to create a decision support system that meets the requirements of decision-makers that coordinate flood disaster response. Two essential requirements are that recommendations for area prioritisation

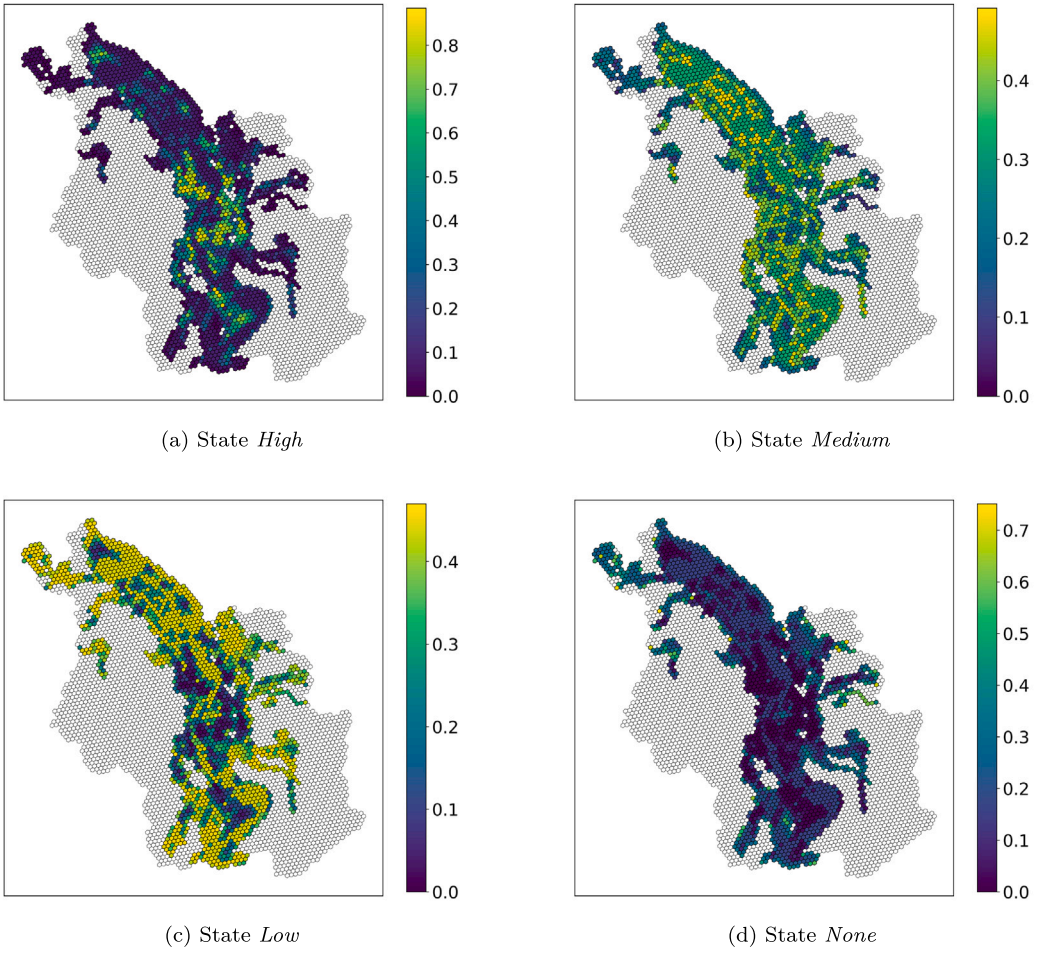

(a) State *High* (b) State *Medium*

(c) State *Low* (d) State *None*

Fig. 10. Results of the GIS-informed BN model.

can be obtained rapidly, since time is usually short, and that the process that leads to these recommendations is transparent, since there is a reluctance to trust black box models in high stake decisions [32,65]. To achieve rapid recommendations, the *PrioReMap* method shifts parts of the decision-making process from the time-critical response phase to the less time-critical preparation phase. Setting up the models (GIS models and BN) prior to an actual disaster can be considered as an early walk-through of the decision-making process that allows stakeholders to identify and discuss relevant variables for prioritisation (the nodes of the BN), including the one that mirrors the response objective (the target node). This approach also makes the process that leads to a recommendation transparent as setting up the BN requires to formalise the reasoning for prioritising certain areas in a comprehensible structure (that is the BN, see also [66] who introduced BNs as a formalism of human reasoning under uncertainty). Another advantage of creating this structure of reasoning before an actual disaster is that it allows to integrate the perspectives of multiple stakeholders and the knowledge of multiple experts (see [67] or [68] for elicitation methods) into the decision-making process, an aspect that is particularly valuable in emergency decision-making, where selection problems are often solved by group decisions [34].

Ultimately, *PrioReMap* combines multiple geospatial variables into a single categorical index that assigns disaster relief priority to every tile. Aggregating several variables into one index is a delicate task that requires careful selection and an appropriate representation of their interplay [69] (e.g., vulnerability without exposure does not result in risk). A BN-based approach was chosen for aggregation into a probability distribution of the risk variable, as BNs provide a logical framework to explicitly model interactions between variables via CPTs. This approach has already proven effective in flood disaster preparedness (see Section 2). To reduce knowledge elicitation effort during BN construction, the number of required probability values was minimised by discretising all variables (e.g., continuous flood depth) and applying an ordered logistic regression model. This facilitates elicitation by defining discrete states (e.g., low flood depth defined as 0.01–0.3 m) and thus significantly reduces the number of probability values required to set up the CPTs. However, discretisation introduces threshold effects: small input changes may cause abrupt probability jumps (e.g., from 100% low to 100% medium). To avoid such effects and improve robustness, we applied a soft evidence approach that distributes probability mass across states. Within future work, optimisation methods for discretisation could be tested, such as the approach by [70] for discretisation of BN variables in rare-event modelling.

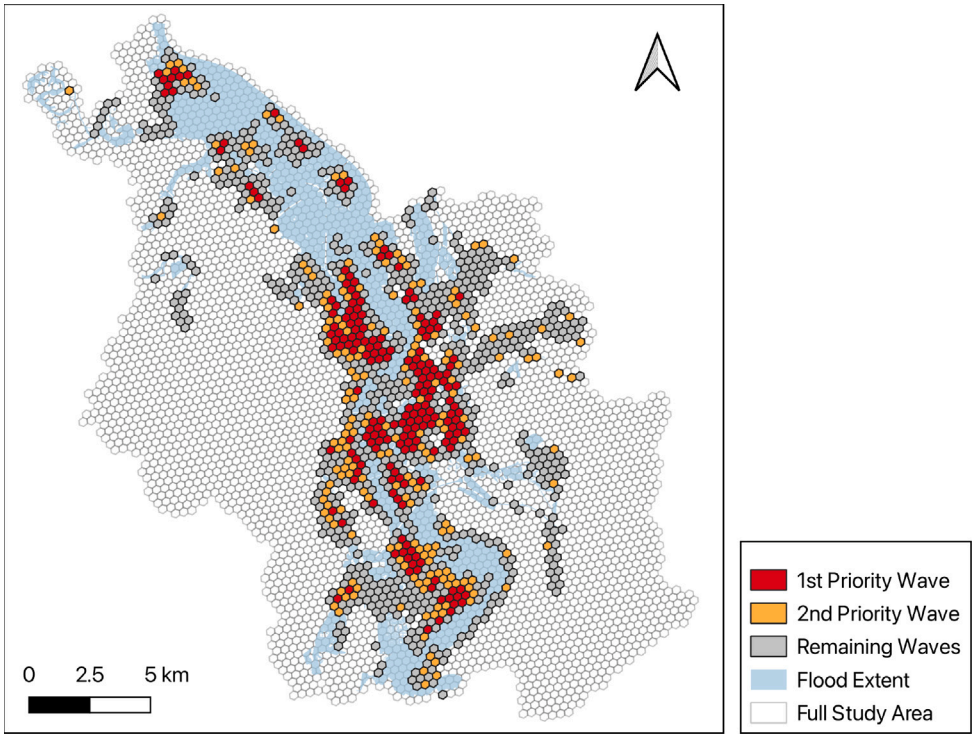

Fig. 11. *PrioReMap* of the case study. In this example visualisation, a wave size of 200 tiles is used. The 1st and 2nd prioritisation waves are shown individually, while the remaining waves are summarised to provide a clearer overview of the most critical tiles. The flood extent is also mapped to support rapid identification of the full flooded area and to facilitate comparison between wave sizes and the flooded area.

During the preparation phase, BN behaviour and the resulting recommendations based on the expected loss method can be explored through case studies using simulated flood scenarios such as the one presented in the case study of this work. Such explorations can and should be applied to tune the model in a way that it reflects the preferences of the responsible disaster responders as well as context-dependent specifics, such as local terrain or available resources. This includes parameters such as the time thresholds used to calculate the expected loss. These thresholds can be set by stakeholder consultations or considering local response protocols, practices, experiences, and hazard dynamics.

In the response phase, however, the allocation-penalty factor ρ becomes most critical, as it allows prioritisation recommendations to be adapted to current resource constraints. The more limited the resources are compared to the affected area, the higher this parameter should be set, since prioritisation must then focus more strongly on avoiding under-allocation in the most critical tiles. Given variations in ρ, sensitivity analysis for the case study demonstrates that the model remains highly robust, particularly for the highest-ranked tiles (see Fig. 12), making it a reliable method for disaster response planning.

In the presented case study, the geospatial data that is required to set up the GIS models is obtained from OSM data – a common source of geospatial data used to support humanitarian disaster relief efforts worldwide [71]. However, if available, data from official government services or critical infrastructure providers is generally preferable as it is typically more accurate and complete [29]. Fortunately, potential end users, such as disaster responders, are likely to have access to this high quality data. When relying on OSM data, potential inaccuracies – such as missing, misplaced, or incorrectly labelled geo-information – must be taken into account [72]. For example, newly constructed roads may be missing from the road network, leading to a false assessment of the accessibility of tiles, or buildings may not be labelled properly, resulting in missing PoIs. Ultimately, such false assessments due to inaccurate data can influence the final area prioritisation recommendations, which is why checking data quality is essential. To address this issue, existing methods for classifying and improving the quality of OSM data can be applied (see, e.g. [73] or [74]). In the end, it is important to emphasise that the effectiveness of *PrioReMap* is directly tied to the quality of the underlying data.

Another essential geospatial data input is the flood hazard layer. While flood inundation is an inherently dynamic phenomenon, we treated it here as a static snapshot within the present case study, using the maximum extent of a simulated flood scenario (HQ500). A limitation of the current method is therefore that the implementation of the flood layer is static. Dynamic flood evolution or live data assimilation is not yet supported. This exemplary inundation layer has the same data structure as layers generated by rapid mapping technologies (see [75] for a step-by-step guide on how to generate such layers using open-source data and tools). The method can in principle be adjusted to display the temporal dynamics of flood inundation by replacing the flood inundation layer at run-time when new information becomes available.

We identified four directions for future research that we consider particularly promising. First, the analysis can be extended to include additional dynamic observations, such as eyewitness reports, emergency calls, or sensor data, which provide further details about the situation during a flood disaster. To achieve this, the *PrioReMap* method could be combined with a method like the *Emergency Response Inference Mapping* method (see [23]), which allows for the integration of dynamic and uncertain or ambiguous observations. The integration of such observations should be carefully discussed with potential end users beforehand, as relying on them for decision making may introduce new uncertainties and hamper accountability. For instance, the absence of emergency calls from a particular area does not necessarily indicate lower urgency — people in those areas may simply lack mobile coverage or access to other communication channels.

Second, an aspect that becomes increasingly relevant when incorporating such additional dynamic observations is the presence of spatial dependencies that can lead to spatial inferences between tiles. For example, if a sensor measures a certain flood depth in one tile, the flood depth in neighbouring tiles could be inferred spatially. For this, given a spatial model predicting flood inundation, a data-assimilation framework can be implemented to combine model predictions with sensor measurements (e.g., see [76]).

Third, the *PrioReMap* could be applied in the context of sectorisation. Sectorisation is a common procedure in the context of emergency relief that organises the disaster region into sectors that require comparable operational demands and thereby allows responders to effectively distribute emergency relief resources (e.g. see [77]). The *PrioReMap* could be integrated in a sectorisation procedure that considers the geographic extent of an area as well as the number of (high) priority tiles within that area.

A limitation of the *PrioReMap* method is that it yet needs to be validated in practice. A fourth aspect of future work is therefore using *PrioReMap* in different scenarios and contexts, and compare the suggested prioritisation against actual operational decisions. Here, both empirical field research during real incidents as well as observational studies during training exercises or serious gaming sessions are promising ways ahead.

7. Conclusion

In this work, we introduced a novel method called Prioritisation Recommendation Mapping (*PrioReMap*) that has the potential to provide rapid and transparent recommendations for area prioritisation in flood disaster response. The benefit of the method is that it allows to shift some of the most time-consuming aspects of the decision-making process from the time-critical response phase to the less time-critical preparation phase. This is achieved as the core of the method is build by a Bayesian network (BN) that includes the different variables that account for flood disaster risk (hazard, exposure, vulnerability) and whose logical structure reflects a comprehensible line of argumentation for prioritising certain areas over others. Ultimately, the output of the method, that is the *PrioReMap*, is obtained from a grid of those BNs. The leaf nodes of these BNs are informed by multiple GIS models that require a flood hazard layer as input. We illustrated the applicability of the *PrioReMap* method in a case study of an extreme flood scenario in the city of Cologne, Germany, showcasing how the method condenses a large volume of spatially explicit information into distinct area prioritisation recommendations. Corresponding recommendations can help decision-makers identify the most at-risk areas in a flood disaster and thus support an effective allocation of scarce resources.

CRediT authorship contribution statement

Moritz Schneider: Writing – review & editing, Writing – original draft, Visualization, Software, Methodology, Conceptualization. **Lukas Halekotte:** Writing – review & editing, Writing – original draft, Supervision, Conceptualization. **Tina Comes:** Writing – review & editing, Supervision, Conceptualization. **Frank Fiedrich:** Writing – review & editing, Supervision, Conceptualization.

Declaration of competing interest

The authors declare that they have no known competing financial interests or personal relationships that could have appeared to influence the work reported in this paper.

Appendix A

A.1. Ordered-logit model parameters

The ordered-logit model requires severity scores x_V for each variable V of the BN (see Table 2), which map categorical states onto the unit interval. In addition, it uses parent weights $w_{C,P}$ that specify the relative influence of a parent variable P on its child C (see Table 3). For each child node $C \in \{\text{Hazard}, \text{Exposure}, \text{Vulnerability}, \text{Risk}\}$, the parameters are identical with $\beta_C = 10$ and cut-points $(\tau_{C,1}, \tau_{C,2}, \tau_{C,3}) = (0.25, 0.50, 0.75)$. Since these variables have $K = 4$ ordered categories (none $\prec$ low $\prec$ medium $\prec$ high), the ordered-logit formulation requires exactly $K - 1 = 3$ cut-points to partition the real line.

Table 2
Variables with their states and corresponding severity scores x_V.

Variable	States	Mapping to $[0, 1]$
Flood Depth	none, shallow, moderate, deep	0.0, 0.33, 0.67, 1.0
Flood Coverage	0%–10%, 10%–50%, >50%	0.0, 0.5, 1.0
Population	none, low, medium, high	0.0, 0.33, 0.67, 1.0
PoI	absent, present	0.0, 1.0
Access Road	accessible, inaccessible	0.0, 1.0
Access Local	accessible, inaccessible	0.0, 1.0
% Elderly	0%–10%, 10%–50%, >50%	0.0, 0.5, 1.0
Hazard	none, low, medium, high	0.0, 0.33, 0.67, 1.0
Exposure	none, low, medium, high	0.0, 0.33, 0.67, 1.0
Vulnerability	none, low, medium, high	0.0, 0.33, 0.67, 1.0

Table 3
Parent weights $w_{C,P}$.

Child	Parent	Weight
Hazard	Flood Depth	0.65
Hazard	Flood Coverage	0.35
Exposure	Population	0.75
Exposure	PoI	0.25
Vulnerability	Access Road	0.40
Vulnerability	Access Local	0.40
Vulnerability	% Elderly	0.20
Risk	Hazard	0.45
Risk	Exposure	0.30
Risk	Vulnerability	0.25

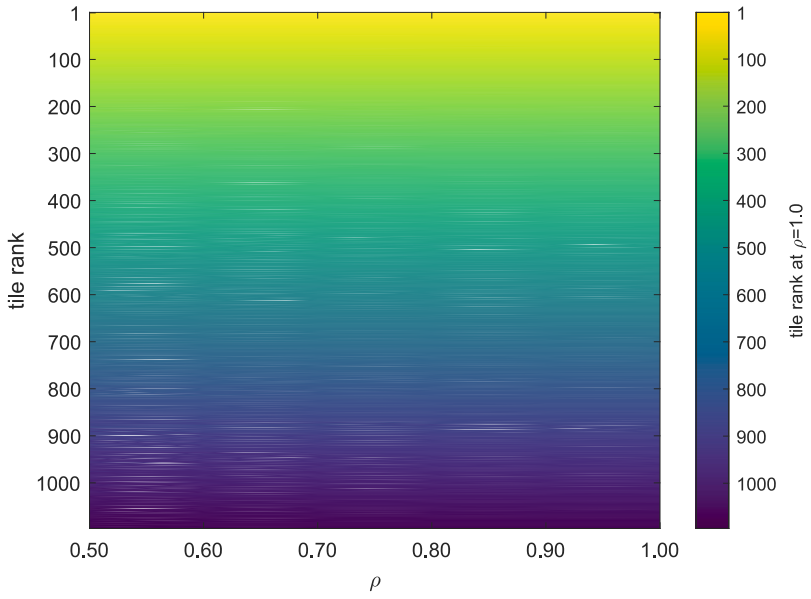

Fig. 12. Robustness of tile ranking with respect to variations in the under- vs. over-allocation penalty ρ. Rank 1 denotes the most critical tile. The results are compared against the baseline in which only under-allocation is penalised ($\rho = 1$, see corresponding spatial distribution in Fig. 13), with ρ varying between 0.5 (equal penalty) and 1 (only under-allocation penalised).

A.2. Sensitivity analysis

The prioritisation method (Section 4.3) is applied to all exposed tiles in the study area, yielding a ranked list of 1096 tiles. To test the robustness of the derived recommendations, we consider how the ranking of the 1096 tiles changes (see Fig. 12) depending on

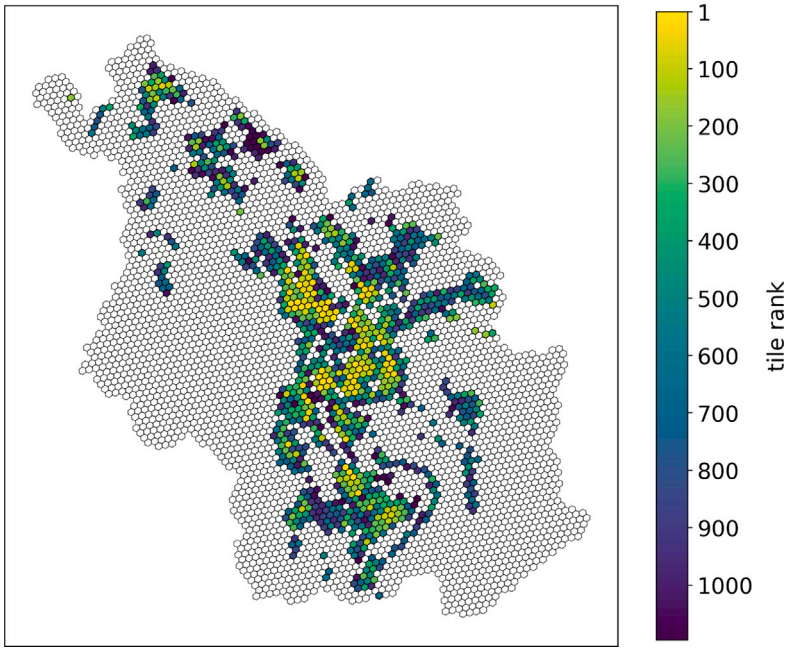

Fig. 13. Tile ranking for $\rho = 1$ for the case study scenario (corresponding to Fig. 12). Rank 1 corresponds to the most critical tile, while Rank 1096 corresponds to the least critical tile in the ranking.

the penalty factor ρ (similar to the procedure outlined in [78]), which governs the relative penalty for under- versus over-allocation. This variable can be considered the key parameter for adjusting the *PrioReMap* to changing resource constraints during the response phase. The changes in the ranking with varying ρ indicate that the recommendations are highly robust (which can be seen by the stable colour coding in Fig. 12), while still allowing for minor adjustments in the tile rankings as ρ varies. The overall correlation between the rankings is pretty high (Spearman's rank correlation of 0.9998 and Kendall's τ of 0.9895 between rankings at $\rho = 1$ and $\rho = 0.5$). Accordingly, the recommendation method shows a robust behaviour, which is especially critical for the highest-priority (most critical) tiles. Considering that tiles are summarised into waves (e.g., waves of 200 tiles), the differences between successive waves can be expected to be even smaller.

Data availability

Data will be made available on request.

References

[1] F.C. Nick, N. Sänger, S. van der Heijden, S. Sandholz, Collaboration is key: Exploring the 2021 flood response for critical infrastructures in germany, Int. J. Disaster Risk Reduct. 91 (2023) 103710, http://dx.doi.org/10.1016/j.ijdrr.2023.103710.
[2] P. Asaridis, D. Molinari, F. Di Maio, F. Ballio, E. Zio, A probabilistic modeling and simulation framework for power grid flood risk assessment, Int. J. Disaster Risk Reduct. 120 (2025) 105353, http://dx.doi.org/10.1016/j.ijdrr.2025.105353.
[3] D.R. Sanderson, T.P. McAllister, Quantifying future local impacts of sea level rise on buildings and infrastructure, Int. J. Disaster Risk Reduct. 127 (2025) 105649, http://dx.doi.org/10.1016/j.ijdrr.2025.105649.
[4] B. Güneralp, İ. Güneralp, Y. Liu, Changing global patterns of urban exposure to flood and drought hazards, Glob. Environ. Chang. 31 (2015) 217–225, http://dx.doi.org/10.1016/j.gloenvcha.2015.01.002.
[5] L. Collet, L. Beevers, M.D. Stewart, Decision-making and flood risk uncertainty: Statistical data set analysis for flood risk assessment, Water Resour. Res. 54 (10) (2018) 7291–7308, http://dx.doi.org/10.1029/2017wr022024.
[6] B. Feng, Y. Zhang, R. Bourke, Urbanization impacts on flood risks based on urban growth data and coupled flood models, Nat. Hazards 106 (1) (2021) 613–627, http://dx.doi.org/10.1007/s11069-020-04480-0.
[7] W. Qi, C. Ma, H. Xu, K. Zhao, Z. Chen, A comprehensive analysis method of spatial prioritization for urban flood management based on source tracking, Ecol. Indic. 135 (2022) 108565, http://dx.doi.org/10.1016/j.ecolind.2022.108565.
[8] C. Ansell, A. Boin, A. Keller, Managing transboundary crises: Identifying the building blocks of an effective response system, J. Contingencies Crisis Manag. 18 (4) (2010) 195–207, http://dx.doi.org/10.1111/j.1468-5973.2010.00620.x.
[9] J.R. Harrald, Agility and discipline: Critical success factors for disaster response, ANNALS Am. Acad. Polit. Soc. Sci. 604 (1) (2006) 256–272, http://dx.doi.org/10.1177/0002716205285404.
[10] J. Son, Z. Aziz, F. Peña-Mora, Supporting disaster response and recovery through improved situation awareness, Struct. Surv. 26 (5) (2008) 411–425, http://dx.doi.org/10.1108/02630800810922757.

[11] C. Armenakis, N. Nirupama, Prioritization of disaster risk in a community using gis, Nat. Hazards 66 (1) (2012) 15–29, http://dx.doi.org/10.1007/s11069-012-0167-8.
[12] M. Wieland, S. Schmidt, B. Resch, A. Abecker, S. Martinis, Fusion of geospatial information from remote sensing and social media to prioritise rapid response actions in case of floods, Nat. Hazards (2025) http://dx.doi.org/10.1007/s11069-025-07120-7.
[13] I. Lapietra, F. Benassi, A. Paterno, T. García-Pereiro, P. Dellino, Mapping social risk areas to floods in southern italy: A spatial analysis for local emergency planning and place-based risk reduction policies, Int. J. Disaster Risk Reduct. 127 (2025) 105666, http://dx.doi.org/10.1016/j.ijdrr.2025.105666.
[14] Y. Lu, G. Zhai, S. Zhou, An integrated bayesian networks and geographic information system (bns-gis) approach for flood disaster risk assessment: A case study of Yinchuan, China, Ecol. Indic. 166 (2024) 112322, http://dx.doi.org/10.1016/j.ecolind.2024.112322.
[15] A. Mentges, L. Halekotte, M. Schneider, T. Demmer, D. Lichte, A resilience glossary shaped by context: Reviewing resilience-related terms for critical infrastructures, Int. J. Disaster Risk Reduct. 96 (2023) 103893, http://dx.doi.org/10.1016/j.ijdrr.2023.103893.
[16] R.B. Mudashiru, N. Sabtu, I. Abustan, W. Balogun, Flood hazard mapping methods: A review, J. Hydrol. 603 (2021) 126846, http://dx.doi.org/10.1016/j.jhydrol.2021.126846.
[17] V. Röthlisberger, A.P. Zischg, M. Keiler, Identifying spatial clusters of flood exposure to support decision making in risk management, Sci. Total Environ. 598 (2017) 593–603, http://dx.doi.org/10.1016/j.scitotenv.2017.03.216.
[18] Y. Casali, N.Y. Aydin, T. Comes, A data-driven approach to analyse the co-evolution of urban systems through a resilience lens: A helsinki case study, Environ. Plan. B: Urban Anal. City Sci. 51 (9) (2024) 2074–2091, http://dx.doi.org/10.1177/23998083241235246.
[19] Y. Alabbad, I. Demir, Understanding flood risk in public transit systems: Insights from accessibility and vulnerability analysis in iowa, Int. J. Disaster Risk Reduct. 126 (2025) 105615, http://dx.doi.org/10.1016/j.ijdrr.2025.105615.
[20] S. Rehman, M. Sahana, H. Hong, H. Sajjad, B.B. Ahmed, A systematic review on approaches and methods used for flood vulnerability assessment: framework for future research, Nat. Hazards 96 (2) (2019) 975–998, http://dx.doi.org/10.1007/s11069-018-03567-z.
[21] T. Comes, Cognitive biases in humanitarian sensemaking and decision-making lessons from field research, in: 2016 IEEE International Multi-Disciplinary Conference on Cognitive Methods in Situation Awareness and Decision Support (CogSIMA), IEEE, 2016, pp. 56–62, http://dx.doi.org/10.1109/cogsima.2016.7497786.
[22] M.A. Thompson Clive, J.M. Lindsay, G.S. Leonard, C. Lutteroth, A. Bostrom, P. Corballis, Volcanic hazard map visualisation affects cognition and crisis decision-making, Int. J. Disaster Risk Reduct. 55 102102. http://dx.doi.org/10.1016/j.ijdrr.2021.102102.
[23] M. Schneider, L. Halekotte, T. Comes, D. Lichte, F. Fiedrich, Emergency response inference mapping (erimap): A bayesian network-based method for dynamic observation processing, Reliab. Eng. Syst. Saf. 255 (2025) 110640, http://dx.doi.org/10.1016/j.ress.2024.110640.
[24] M. Sirenko, T. Comes, A. Verbraeck, The rhythm of risk: Exploring spatio-temporal patterns of urban vulnerability with ambulance calls data, Environ. Plan. B: Urban Anal. City Sci. 52 (4) (2024) 863–881, http://dx.doi.org/10.1177/23998083241272095.
[25] B. Van de Walle, B. Brugghemans, T. Comes, Improving situation awareness in crisis response teams: An experimental analysis of enriched information and centralized coordination, Int. J. Hum.-Comput. Stud. 95 (2016) 66–79, http://dx.doi.org/10.1016/j.ijhcs.2016.05.001.
[26] T. Comes, Ai for crisis decisions, Ethics Inf. Technol. 26 (1) (2024) http://dx.doi.org/10.1007/s10676-024-09750-0.
[27] V. Zwirglmaier, M. Garschagen, Linking urban structure types and bayesian network modelling for an integrated flood risk assessment in data-scarce mega-cities, Urban Clim. 56 (2024) 102034, http://dx.doi.org/10.1016/j.uclim.2024.102034.
[28] Z. Wu, Y. Shen, H. Wang, M. Wu, Assessing urban flood disaster risk using bayesian network model and gis applications, Geomatics, Nat. Hazards Risk 10 (1) (2019) 2163–2184, http://dx.doi.org/10.1080/19475705.2019.1685010.
[29] M. Schneider, L. Halekotte, A. Mentges, F. Fiedrich, Dependent infrastructure service disruption mapping (disruptionmap): A method to assess cascading service disruptions in disaster scenarios, Sci. Rep. 15 (1) (2025) http://dx.doi.org/10.1038/s41598-025-89469-0.
[30] M. Kanti Sen, S. Dutta, An integrated gis-bbn approach to quantify resilience of roadways network infrastructure system against flood hazard, ASCE-ASME J. Risk Uncertain. Eng. Syst. Part A: Civ. Eng. 6 (4) (2020) http://dx.doi.org/10.1061/ajrua6.0001088.
[31] M. Druzdzel, L. van der Gaag, Building probabilistic networks: Where do the numbers come from? guest editors' introduction, IEEE Trans. Knowl. Data Eng. 12 (4) (2000) 481–486, http://dx.doi.org/10.1109/TKDE.2000.868901.
[32] C.-C. Lee, T. Comes, M. Finn, A. Mostafavi, Roadmap towards responsible ai in crisis resilience management, 2022, http://dx.doi.org/10.48550/ARXIV.2207.09648.
[33] J. Pearl, Bayesian networks: A model of self-activated memory for evidential reasoning, in: Proceedings of the 7th Conference of the Cognitive Science Society, University of California, Irvine, CA, USA, 1985, pp. 15–17.
[34] J. Zheng, Y. Wang, K. Zhang, J. Liang, A dynamic emergency decision-making method based on group decision making with uncertainty information, Int. J. Disaster Risk Sci. 11 (5) (2020) 667–679, http://dx.doi.org/10.1007/s13753-020-00308-4.
[35] Y. Zhang, B.K. Teoh, L. Zhang, Integrated bayesian networks with gis for electric vehicles charging site selection, J. Clean. Prod. 344 (2022) 131049, http://dx.doi.org/10.1016/j.jclepro.2022.131049.
[36] S. Ali, R.A. Stewart, O. Sahin, A.S. Vieira, Spatial bayesian approach for socio-economic assessment of pumped hydro storage, Renew. Sustain. Energy Rev. 189 (2024) 114007, http://dx.doi.org/10.1016/j.rser.2023.114007.
[37] Z. Xu, S. Zhou, C. Zhang, M. Yang, M. Jiang, A bayesian network model for suitability evaluation of underground space development in urban areas: The case of Changsha, China, J. Clean. Prod. 418 (2023) 138135, http://dx.doi.org/10.1016/j.jclepro.2023.138135.
[38] J. Gonzalez-Redin, S. Luque, L. Poggio, R. Smith, A. Gimona, Spatial bayesian belief networks as a planning decision tool for mapping ecosystem services trade-offs on forested landscapes, Environ. Res. 144 (2016) 15–26, http://dx.doi.org/10.1016/j.envres.2015.11.009.
[39] W.M. Dlamini, Application of bayesian networks for fire risk mapping using gis and remote sensing data, GeoJournal 76 (3) (2010) 283–296, http://dx.doi.org/10.1007/s10708-010-9362-x.
[40] A. Grêt-Regamey, D. Straub, Spatially explicit avalanche risk assessment linking bayesian networks to a gis, Nat. Hazards Earth Syst. Sci. 6 (6) (2006) 911–926, http://dx.doi.org/10.5194/nhess-6-911-2006.
[41] K. Guo, X. Zhang, X. Kuai, Z. Wu, Y. Chen, Y. Liu, A spatial bayesian-network approach as a decision-making tool for ecological-risk prevention in land ecosystems, Ecol. Model. 419 (2020) 108929, http://dx.doi.org/10.1016/j.ecolmodel.2019.108929.
[42] E. Arango, M. Santamaria, M. Nogal, H.S. Sousa, J.C. Matos, Flood risk assessment for road infrastructures using bayesian networks: case study of santarem - portugal, Acta Polytech. CTU Proc. 36 (2022) 33–46, http://dx.doi.org/10.14311/app.2022.36.0033.
[43] S. Huang, H. Wang, Y. Xu, J. She, J. Huang, Key disaster-causing factors chains on urban flood risk based on bayesian network, Land 10 (2) (2021) 210, http://dx.doi.org/10.3390/land10020210.
[44] S. Balbi, F. Villa, V. Mojtahed, K.T. Hegetschweiler, C. Giupponi, A spatial bayesian network model to assess the benefits of early warning for urban flood risk to people, Nat. Hazards Earth Syst. Sci. 16 (6) (2016) 1323–1337, http://dx.doi.org/10.5194/nhess-16-1323-2016.
[45] K. Sahr, Hexagonal discrete global grid systems for geospatial computing, Arch. Fotogram. Kartogr. I Teledetekcji 22 (2011) 363–376.
[46] A. Kmoch, I. Vasilyev, H. Virro, E. Uuemaa, Area and shape distortions in open-source discrete global grid systems, Big Earth Data 6 (3) (2022) 256–275, http://dx.doi.org/10.1080/20964471.2022.2094926.
[47] A. Maranzoni, M. D'Oria, C. Rizzo, Quantitative flood hazard assessment methods: A review, J. Flood Risk Manag. 16 (1) (2022) http://dx.doi.org/10.1111/jfr3.12855.

[48] B. Li, J. Hou, X. Wang, Y. Ma, D. Li, T. Wang, G. Chen, High-resolution flood numerical model and dijkstra algorithm based risk avoidance routes planning, Water Resour. Manag. 37 (8) (2023) 3243–3258, http://dx.doi.org/10.1007/s11269-023-03500-5.
[49] U. Gangwal, A.R. Siders, J. Horney, H.A. Michael, S. Dong, Critical facility accessibility and road criticality assessment considering flood-induced partial failure, Sustain. Resilient Infrastruct. 8 (sup1) (2022) 337–355, http://dx.doi.org/10.1080/23789689.2022.2149184.
[50] OpenStreetMap contributors, 2017, Planet dump retrieved from https://planet.osm.org, https://www.openstreetmap.org.
[51] H.-K. Lee, W.-H. Hong, Y.-H. Lee, Experimental study on the influence of water depth on the evacuation speed of elderly people in flood conditions, Int. J. Disaster Risk Reduct. 39 (2019) 101198, http://dx.doi.org/10.1016/j.ijdrr.2019.101198.
[52] M. Yazdani, M. Haghani, Elderly people evacuation planning in response to extreme flood events using optimisation-based decision-making systems: A case study in Western Sydney, Australia, Knowl.-Based Syst. 274 (2023) 110629, http://dx.doi.org/10.1016/j.knosys.2023.110629.
[53] B. Sahoh, A. Choksuriwong, The role of explainable artificial intelligence in high-stakes decision-making systems: a systematic review, J. Ambient. Intell. Humaniz. Comput. 14 (6) (2023) 7827–7843, http://dx.doi.org/10.1007/s12652-023-04594-w.
[54] F. Rijmen, Bayesian networks with a logistic regression model for the conditional probabilities, Internat. J. Approx. Reason. 48 (2) (2008) 659–666, http://dx.doi.org/10.1016/j.ijar.2008.01.001.
[55] A. Lannoy, H. Procaccia, Expertise, safety, reliability, and decision making: practical industrial experience, Environ. Syst. Decis. 34 (2) (2014) 259–276, http://dx.doi.org/10.1007/s10669-014-9500-y.
[56] X. Jiang, S. Mahadevan, Bayesian risk-based decision method for model validation under uncertainty, Reliab. Eng. Syst. Saf. 92 (6) (2007) 707–718, http://dx.doi.org/10.1016/j.ress.2006.03.006.
[57] M. Bosmans, C. Baliatsas, C. Yzermans, M. Dückers, A systematic review of rapid needs assessments and their usefulness for disaster decision making: Methods, strengths and weaknesses and value for disaster relief policy, Int. J. Disaster Risk Reduct. 71 (2022) 102807, http://dx.doi.org/10.1016/j.ijdrr.2022.102807, https://www.sciencedirect.com/science/article/pii/S2212420922000267.
[58] E. Gralla, J. Goentzel, B. Van de Walle, A. Verity, Report from the workshop on field-based decision makers' information needs in sudden onset disasters, Tech. rep., ACAPS & UN OCHA, workshop report, 2013, https://www.academia.edu/19454748/Report_from_the_Workshop_on_Field_Based_Decision_Makers_Information_Needs_in_Sudden_Onset_Disasters.
[59] A. Fink, U. Ulbrich, H. Engel, Aspects of the January 1995 flood in Germany, Weather 51 (2) (1996) 34–39, http://dx.doi.org/10.1002/j.1477-8696.1996.tb06182.x.
[60] B. Merz, H. Kreibich, R. Schwarze, A. Thieken, Review article assessment of economic flood damage, Nat. Hazards Earth Syst. Sci. 10 (8) (2010) 1697–1724, http://dx.doi.org/10.5194/nhess-10-1697-2010.
[61] M. Bier, R. Fathi, C. Stephan, A. Kahl, F. Fiedrich, A. Fekete, Spontaneous volunteers and the flood disaster 2021 in Germany: Development of social innovations in flood risk management, J. Flood Risk Manag. (2023) http://dx.doi.org/10.1111/jfr3.12933.
[62] F. Müller, M. Bier, S. Tomczyk, A. Kahl, F. Fiedrich, The issue of overload: A mixed methods analysis of activity-related stress and the use of mental health and psychosocial support by spontaneous volunteers during the 2021 flood in Germany, Int. J. Disaster Risk Reduct. (2025) 105534, http://dx.doi.org/10.1016/j.ijdrr.2025.105534.
[63] State Agency for Nature, Environment and Consumer Protection of North Rhine-Westphalia, INSPIRE Dataset Feed: Flood risk map Layer NRW - Low probability (HQ500), 2024, (Accessed 09.04.2024). https://www.gis-rest.nrw.de/atomFeed/rest/atom/182925c1-879f-4054-bd69-b6f28e05b270.html.
[64] A. Fekete, Critical infrastructure cascading effects, Disaster resilience assessment for floods affecting city of Cologne and Rhein-Erft-Kreis, J. Flood Risk Manag. 13 (2) (2020) e312600, http://dx.doi.org/10.1111/jfr3.12600.
[65] A. de Waal, J.W. Joubert, Explainable Bayesian networks applied to transport vulnerability, Expert Syst. Appl. 209 (2022) 118348, http://dx.doi.org/10.1016/j.eswa.2022.118348.
[66] J. Peal, Bayesian networks: A model of self-activated memory for evidential reasoning, in: Proceedings of the Annual Meeting of the Cognitive Science Society, vol. 7, 1985.
[67] K.L. Hassall, G. Dailey, J. Zawadzka, A.E. Milne, J.A. Harris, R. Corstanje, A.P. Whitmore, Facilitating the elicitation of beliefs for use in Bayesian Belief modelling, Environ. Model. Softw. 122 (2019) 104539, http://dx.doi.org/10.1016/j.envsoft.2019.104539.
[68] D.E. Morris, J.E. Oakley, J.A. Crowe, A web-based tool for eliciting probability distributions from experts, Environ. Model. Softw. 52 (2014) 1–4, http://dx.doi.org/10.1016/j.envsoft.2013.10.010.
[69] L. Halekotte, A. Mentges, D. Lichte, Do we practice what we preach? the dissonance between resilience understanding and measurement, Int. J. Disaster Risk Reduct. 118 (2025) 105265, http://dx.doi.org/10.1016/j.ijdrr.2025.105265.
[70] K. Zwirglmaier, D. Straub, A discretization procedure for rare events in Bayesian networks, Reliab. Eng. Syst. Saf. 153 (2016) 96–109, http://dx.doi.org/10.1016/j.ress.2016.04.008, https://www.sciencedirect.com/science/article/pii/S0951832016300229.
[71] B. Herfort, S. Lautenbach, J. Porto de Albuquerque, J. Anderson, A. Zipf, The evolution of humanitarian mapping within the openstreetmap community, Sci. Rep. 11 (1) (2021) http://dx.doi.org/10.1038/s41598-021-82404-z.
[72] J. Kaur, J. Singh, S.S. Sehra, H.S. Rai, Systematic literature review of data quality within openstreetmap, in: 2017 International Conference on Next Generation Computing and Information Systems, ICNGCIS, IEEE, 2017, pp. 177–182, http://dx.doi.org/10.1109/icngcis.2017.35.
[73] M.A. Brovelli, G. Zamboni, A new method for the assessment of spatial accuracy and completeness of openstreetmap building footprints, ISPRS Int. J. Geo-Inform. 7 (8) (2018) 289, http://dx.doi.org/10.3390/ijgi7080289.
[74] F. Biljecki, Y.S. Chow, K. Lee, Quality of crowdsourced geospatial building information: A global assessment of openstreetmap attributes, Build. Environ. 237 (2023) 110295, http://dx.doi.org/10.1016/j.buildenv.2023.110295.
[75] UN-SPIDER, Recommended practice: Flood mapping and damage assessment using sentinel-2 (s2) optical data, 2025, (Accessed: 2025-06-16). https://www.un-spider.org/advisory-support/recommended-practices.
[76] M.G. Ziliani, R. Ghostine, B. Ait-El-Fquih, M.F. McCabe, I. Hoteit, Enhanced flood forecasting through ensemble data assimilation and joint state-parameter estimation, J. Hydrol. 577 (2019) 123924, http://dx.doi.org/10.1016/j.jhydrol.2019.123924.
[77] UN-OCHA, INSARAG Guidelines Volume II, Manual B: Operations, United Nations Office for the Coordination of Humanitarian Affairs, Geneva, Switzerland, 2020, https://www.insarag.org.
[78] L. Halekotte, A. Vanselow, U. Feudel, Keep the bees off the trees: the vulnerability of species in the periphery of mutualistic networks to shock perturbations, J. Phys.: Complex. 6 (3) (2025) 035002, http://dx.doi.org/10.1088/2632-072x/ade927.